3.1 Introduction

With our interest in identifying a solid electrolyte of good electrical conductivity and capacitance values, we first explored the traditional melt-quench prepared glass systems. Even though the results are not very encouraging with these materials we report in this chapter the experimental observations in this regard.

Heavy metal oxide glasses are well known for their special features such as (i) being transparent to wide spectral range and (ii) having the potential for radiation shielding. They are also known for their specific optical properties [1]. Lead oxide (PbO) derived glasses have their importance due to their low melting temperature. Primarily, PbO was hosted in silicate glass, which reduces the temperature of silicate glass formation. Lead oxide glasses have been widely explored with silicate, borate and phosphate systems [2]. PbO has its distinguished role in glass formation depending on its concentration [3]. Electrical conductivity studies on PbO-$PbCl_2$ glasses were also reported [4, 5].

Nature of bonding in the glass matrix depends on the type of bonding (ionic or covalent) between lead and oxygen. Dual nature of PbO helps in stable and transparent glass formation readily with a low crystallization rate. PbO can be a glass network former or a modifier in glassy system. Outermost two electrons of Pb^{+2} ion makes it highly polarizable; this helps in the formation of glass network without destructing the three-dimensional metal oxide framework. Bonding nature of Pb in lead glasses depends on its available concentration. For higher concentration of PbO, Pb–O bonds are covalent and helps in forming 3D-glass network i.e. it acts as a network forming oxide. Pb^{+2} ions <80% has ionic bonding and for >50% Pb^{+2} ions it has covalent bonding between Pb and O atoms [6, 7]. Raman studies confirms that for higher PbO concentration, Pb^{+2} enters into the glass network as a former in form of PbO_4 pyramidal units [8]. Increase in PbO concentration, increases the number of non-bridging oxygen in the network which weakens the cohesion energy of glass network with loosely bounded Pb^{+2} ions [9].

Pb^{+2} ions have been doped in different glass forming units and its distinguished role has been determined by different spectroscopic investigations. Doping of lead ions into the glass network affects coordination geometry of the ions present in the network, in terms of variation in their properties. $PbCl_2$ being ionic in nature, introduces ionic bonding character in the network, making PbO-$PbCl_2$ derived glasses ionic [10]. Several reports

focus on the addition of rare earth ions in lead glasses. For example, doping of Nd_2O_3 improves photo-luminescence properties of these glasses, whereas Eu_2O_3 doping brings in the glass transition temperature changes before and after electron beam treatments [11, 12].

Lead glasses have their importance for ionic conduction properties. With these composites, most of the work has been done on the surface and ionic conductivity. Lead glasses in general are non-conducting/very poorly conducting at room temperature (σ ~10^{-14} to 10^{-10} Ω^{-1} cm^{-1}) whereas at high temperature they exhibit conductivity (σ) around ~10^{-7} to 10^{-6} Ω^{-1} cm^{-1} [13]. According to literature findings, PbO-PbX_2 (X= Cl, F, Br, I) systems have been explored along with B_2O_3 and P_2O_5, majorly for ion transport [14]. Apart from glass-forming network, B_2O_3 also helps in ion transport due to electron deficient nature of Boron as well as the formation of ring-like structure that helps in ion transport mechanism. In similar systems, cation (Pb^{+2}) and anions (oxide and chloride ion) conductance has been reported [4].

NMR, XPS [15], IR and Raman [16, 17] investigations have been done mostly to understand the local order and characterization of lead oxide and lead halides bonding in silicate, borate and phosphate glasses. Based on our findings and best to our knowledge, lead-based glasses lack in their systematic studies for structure and property correlations.

Substitution of cadmium in place of lead was of interest to understand and explore the effect of Cd^{+2} incorporation in the glassy network. Cadmium being almost similar in size (covalent radii-144 pm) compared to Lead (covalent radii-146 pm) can possibly fit in the amorphous system with same glass forming characters, with minor structural variations in the system. Reports on cadmium derived superionic materials, conveys interesting ionic conducting properties and are useful as a transparent glass in photonics [13]. Jie F. *et al.* [18] explored the formation of glass in PbO-$PbCl_2$-$CdCl_2$ systems. Montagne et al. by NMR and XPS technique [15] further explored this system for coordination of Pb and Cd ions. The glasses that have a high amount of chlorine and lead are polarized easily, and this makes these systems conductive in nature. Structure of these glasses has $Pb_3O_2Cl_2$ (mendipite) like crystalline units, consisting of $[O_2Pb_3]^{+2}$ chains formed by edge shared oxo-centered OPb_4 tetrahedra. These chains are unidirectional and are linked together by chlorine atoms present in between the chains. ^{113}Cd NMR of this system

reported for Cd being present in the three-dimensional network via Cd-Cl bond formation. The first representative of mixed Pb-Cd oxyhalides in $PbO\text{-}PbCl_2\text{-}CdO$ system is $CdPb_2O_2Cl_2$ [20]. According to the crystal structural investigations of $CdPb_2O_2Cl_2$, Pb^{+2} ions are coordinated by three O^{-2} and five Cl^- anions, with distorted polyhedron and the presence of $6s^2$ lone pair, makes it reasonable for spectro-chemical activities. On the other side, Cd^{+2} has symmetric coordination geometry with two Cd-O bonds and four Cd-Cl bonds by forming CdO_2Cl_4 octahedron. In the oxo-centered heterometallic OPb_3Cd unit, each oxygen atom is coordinated to three Pb^{+2} and one Cd^{+2} cation. Average bond length of O-metal is 2.28 Å and for metal-metal bond, it is 3.72 Å. In pure OPb_4 tetrahedron, bond length is 2.33 Å. In OPb_3Cd unit, bond lengths are less than OPb_4 due to the substitution of Pb by Cd in an oxo-centered tetrahedron. In glassy composites of these systems, chains are present in form of $[O_2Pb_2Cd]^{+2}$ layers, joined together by equatorial cadmium atom; chloride ions lie above the oxo-centered cavities. Alemi *et al.* further explored, cadmium doped lead borate glasses and concludes for no significant change in the 3D arrangement of the glassy network due to the presence of cadmium in the system [17].

Addition of Cu^{+2} ions into the glass network effects the neighboring inorganic ions in the glassy network by modifying the network [16, 20]. In $PbO\text{-}PbCl_2\text{-}CuCl_2$ composites, Cu^{+2} is present in octahedral coordination in form of CuO_xCl_y (CuO_4Cl_2) polyhedra. Bonding nature of copper is determined by the amount of network former or modifier, size of ions, glass structure, field strength etc. present in the system. Hence, interesting electrical, optical and magnetic properties are imparted along with an increase in chemical resistance thereby strengthening the glassy network due to the addition of Cu^{+2} ions. Presence of Cu^{+2} ions even make the sample sensitive to magnetic resonance spectroscopy which further helps to explore and understand the structural properties of glassy samples through EPR. The structure of some ternary $PbO\text{-}PbCl_2\text{-}CuCl_2$ glasses were studied by Raghunathan *et al.* by EPR and ESEM studies and it was reported that in these glass systems Cu^{2+} exists in a wide variety of geometries each one differing slightly from the other and the overall population following a statistical distribution [21, 22].

In the present work, structure and properties have been explored for some of these systems (PbO-$PbCl_2$-$CuCl_2$ glass systems with Li_2O, $CdCl_2$ and CdO substitution) through electrical transport and thermal studies.

Following systems were explored for the same:

1. **System 3A:** xLi_2O-$(70-x)PbO$-$20.5PbCl_2$-$0.5CuCl_2$; (LPC series)
   x = 1, 5, 10, 15, 20, 40 mol%
2. **System 3B:** $xCdO$-$(80-x)PbO$-$20PbCl_2$; (CPP series)
   x = 5, 10, 15, 20, 30 mol%
3. **System 3C:** $xCdO$- $(80-x)PbO$-$19PbCl_2$-$CuCl_2$; (CPPC series)
   x = 5, 10, 15, 20, 30 mol%
4. **System 3D:** xLi_2O-$(50-x)PbO$-$19PbCl_2$-$30CdO$-$CuCl_2$; (LPCC series)
   x = 1, 5, 10, 15, 20, 30 mol%

Structure and property correlation of the prepared systems has been done through different techniques like XRD, EPR, DSC, TGA, IR and temperature dependent conductivity measurements. Apart from these, some other physical properties have also been calculated and investigated to understand these systems (Table 3.1).

Table 3.1: Composition, Density and Molar volume of the prepared Lead Oxyhalide Glasses.

Sample Code	Li_2O	PbO	$PbCl_2$	$CuCl_2$	CdO	$CdCl_2$	Density ($g\ cm^{-3}$)	Molar Volume ($cm^3\ mol^{-1}$)	
	(mol%)						Experim-ental	Experim-ental	Calculat-ed
System 3A: xLi_2O-$(70-x)PbO$-$20.5PbCl_2$-$0.5CuCl_2$ (LPC series)									
1LPC	1	69	29.5	0.5	0	0	6.635	35.72	28.42
5LPC	5	65	29.5	0.5	0	0	4.447	51.56	28.52
10LPC	10	60	29.5	0.5	0	0	4.327	50.76	28.66
15LPC	15	55	29.5	0.5	0	0	4.281	49.04	28.81
20LPC	20	50	29.5	0.5	0	0	3.909	51.24	28.98
40LPC	40	30	29.5	0.5	0	0	3.422	53.75	28.92
System 3B: $xCdO$-$(80-x)PbO$-$20PbCl_2$; (CPP series)									
PP	0	80	20	0	00	0	5.527	43.36	26.63
5CPP	0	75	20	0	05	0	5.195	44.16	27.07

Sample Code	Li_2O	PbO	$PbCl_2$	$CuCl_2$	CdO	$CdCl_2$	Density ($g\ cm^{-3}$)	Molar Volume ($cm^3\ mol^{-1}$)	
	(mol%)						Experim-ental	Experim-ental	Calculat-ed
10CPP	0	70	20	0	10	0	4.918	45.68	27.55
15CPP	0	65	20	0	15	0	4.906	44.83	28.06
20CPP	0	60	20	0	20	0	4.441	48.45	28.63
30CPP	0	50	20	0	30	0	4.331	47.50	29.90
System 3C: xCdO- (80-x)PbO-19$PbCl_2$-$CuCl_2$; (CPPC series)									
PPC	0	80	19	1	00	0	4.458	52.20	26.54
5CPPC	0	75	19	1	05	0	3.338	68.29	26.98
10CPPC	0	70	19	1	10	0	3.338	66.86	27.45
15CPPC	0	65	19	1	15	0	3.207	68.14	27.97
20CPPC	0	60	19	1	20	0	2.225	96.07	28.53
30CPPC	0	50	19	1	30	0	4.329	47.18	29.80
System 3D: xLi_2O-(50-x)PbO-19$PbCl_2$-30CdO-$CuCl_2$; (LPCC series)									
LPCC	1	49	19	1	30	0	4.801	42.15	29.85
5LPCC	5	45	19	1	30	0	4.335	44.89	30.04
10LPCC	10	40	19	1	30	0	4.199	44.05	30.30
15LPCC	15	35	19	1	30	0	3.949	44.39	30.60
20LPCC	20	30	19	1	30	0	3.625	45.69	30.95
30LPCC	30	20	19	1	30	0	3.558	41.12	31.80

3.2 Composition Accuracy

Compositions of the prepared samples have been checked for their compositional accuracy by estimating the concentration of lead as lead chromate via the standard gravimetric procedure (explained in chapter 2). The results from the gravimetric analysis are in good agreement with the planned compositions for all the series.

3.3 Structural Characterization

These composites do not exhibit much encouraging results for ionic conductivity of these glassy materials. Very poor and not reproducible conductivity values are observed for system 3A-C. A detailed study on structure and properties has been shown only for

system 3D glass composites, as these compositions have substitution of Li^+ ions and are expected to show some measurable conductivity. This system also includes CdO and hence the understanding the electrical conductivity phenomenon along with corresponding structural changes will be interesting.

3.3.1 Density and Molar Volume

Density and molar volume of LPCC composites has been determined (Table 3.1). Molar volume of the sample increases for the substitution of lithium oxide, as it modifies the network by changing the bonding nature of lead present in PbO_4 pyramidal units. Decrease in density and the consequent increase in the molar volume of the samples with lithium oxide addition are due to the expansion of glass structure which becomes more open and flexible.

3.3.2 Powder X-Ray Diffraction

Powder X-ray diffraction of all the prepared composites exhibited hallow pattern conforming for their amorphous/glassy nature (Fig. 3.1). The complete absence of diffraction peaks from the samples scans up to x = 30 mol% lithium oxide (maximum amount added) substitution exhibits halo pattern and confirms amorphous nature in a wide range of compositions.

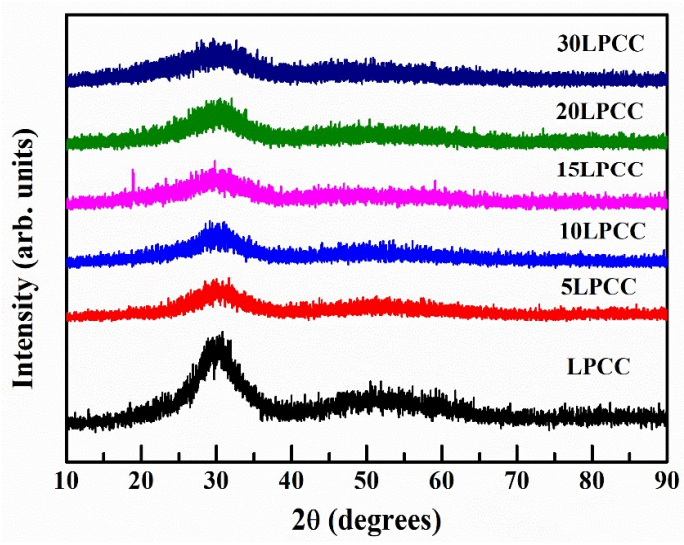

Fig. 3.1 PXRD scan of LPCC series.

3.3.3 Powder X-Ray Diffraction of Annealed Samples

Annealing of samples at multiple crystallization temperatures (obtained from DSC scans) leads to precipitation of different lead and cadmium compounds with respect to their crystallization temperature (Fig. 3.2). LPCC series was initially annealed at first crystallization temperature (T_{c1}) ~400 ºC mainly lead to precipitation of PbO and $PbCl_2$ in form of $Pb_3O_2Cl_2$. 10LPCC sample seems to be not properly annealed at 400 °C; considering this as an experimental error we can analyze the other results. Reannealing of the samples at second crystallization temperature (T_{c2}) ~500 °C lead to complete precipitation of some cadmium composites along with PbO and $PbCl_2$ salts some viz; $Pb_5O_2Cl_6$, $CdPb_2O_5$, Li_4O_4Pb, $Pb_4O_3Cl_2$, PbO_2Cl_2, and Cd_2PbO_4 irrespective of their composition. These samples after annealing at crystallization temperature no more retain their amorphous nature and were transformed into crystalline phases.

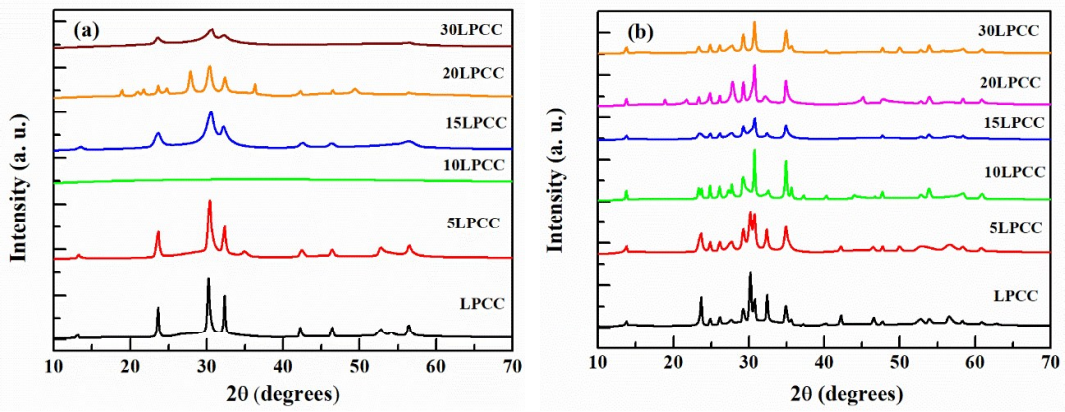

Fig. 3.2 PXRD of LPCC series annealed at (a) 400 °C, and (b) 500 °C.

Table 3.2 - Precipitated particulate size (nm) after annealing at different crystallization temperature (with error of ±2 nm).

Sample Code	350 °C	400 °C	450 °C
1LPCC	317	288	341
5LPCC	207	140	260
10LPCC	-	281	444
15LPCC	138	125	271
20LPCC	76	-	200
30LPCC	68	-	314

The particle size of the precipitated composites in glassy samples has been calculated

using Debye-Scherer formula by using FWHM of the XRD peaks. For example, LPCC sample heated for 5 hours at 330 ^{o}C leads to precipitation of particulate size of approximately 15 (±2) nm. Size of the particulates increases with increase in temperature and time of annealing i.e. for annealing at 475 ^{o}C particulate size of 27 (±2) nm is obtained.

3.3.4 Electron Paramagnetic Resonance Spectroscopy

Addition of $CuCl_2.5H_2O$ (1 mol%) in LPCC series contained Cu^{+2} as a paramagnetic nucleus, which makes the samples EPR active. Copper has two naturally occurring isotopes ^{63}Cu (abundance 69.1%) and ^{65}Cu (abundance 30.9%). For both the isotopes Cu^{+2} ($3d^9$ configuration) has S = ½ and I = 3/2. This makes Cu^{+2} ion paramagnetic and sensitive to EPR experiment. Four parallel and four perpendicular hyperfine lines are expected in an axial symmetry case. Fig. 3.3 shows the characteristic Cu^{+2} hyperfine splitting clearly in X-band region, which gets merged up in Q-band scans (room temperature).

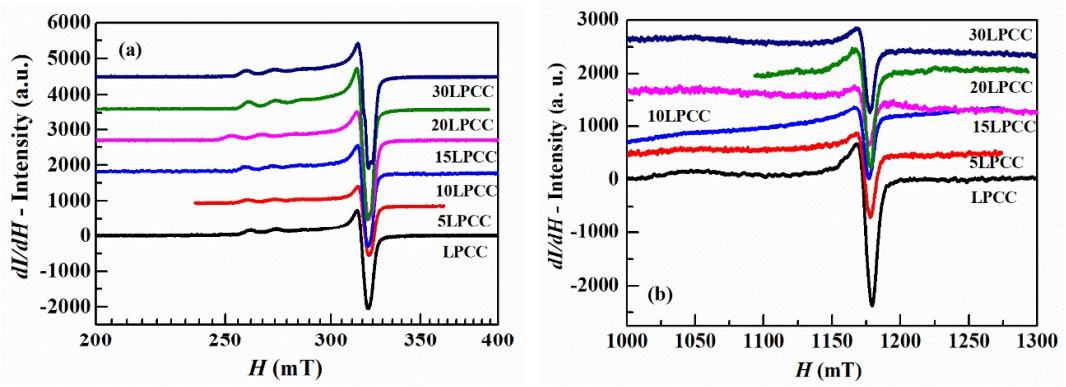

Fig. 3.3 EPR spectra of LPCC series (a) X-band, and (b) Q-band region.

The resolution of hyperfine splitting in low frequency (X-band) and broadening at high frequency (Q-band) is expected for systems where bonding parameters are distributed. A distribution of g and A values expected as a consequence. The spectral simulations based on the model explained in Chapter 2 reveal $g_{\parallel}$, $g_{\perp}$ distribution can be explained in terms of bivariate normal density function. Practically it means cupric ion's geometry varies slightly from site to site. Distribution in $A_{\parallel}$, $A_{\perp}$ is not significant.

3.3.5 FTIR Spectroscopy

Heavy metal oxides such as PbO in pure form do not exhibit IR bands in IR region of 500 - 4000 cm^{-1}. For PbO derived glasses, IR bands can be observed in the frequency range of 450 - 850 cm^{-1} and bands of 1396 cm^{-1} region [23]. These IR bands are for certain possible impurities like lead orthosilicate ($PbSiO_4$) present in the system at the time of preparations. IR bands for vibration of Pb-O unit appear only in far-IR region i.e. below 400 cm^{-1} and around 140 cm^{-1}. For the present work, IR spectrum in Fig. 3.4 showed the glasses to be mostly transparent in the IR region. The suppressed frequency band of 1718 cm^{-1} corresponds to vibrations of Pb-O bonds. Bonds corresponding to –O-Pb-O- bridging are not visible in the spectrum at ~3436 cm^{-1}. For concentrations of PbO > 45 mol%, IR bands in the region of 460 cm^{-1} and 470 cm^{-1} are observed. These bands relate to the concentration of PbO i.e. with increased concentration of PbO intensity of these bands increases with a shift of center to lower wavenumber. This is particularly due to measured dislocation of Pb^{+2} ions from tetrahedral position to octahedral position. Intense IR bands corresponding to pure $PbCl_2$ are present in the region of 2850 – 2950 cm^{-1} [24]. Although the structure of glass differs completely from pure substance. However, the small amount of $PbCl_2$ is still present in the glassy samples.

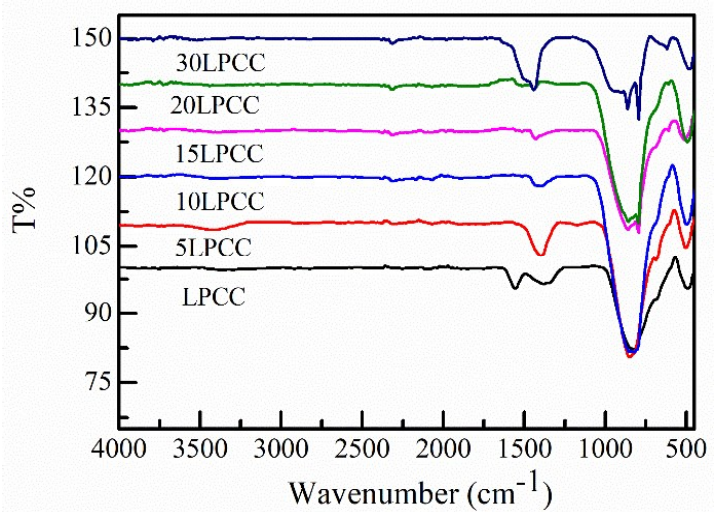

Fig. 3.4 FTIR spectrum of the composites.

Addition of $CuCl_2$ in the composition may also result in the formation of a small amount of CuO into the glass matrix [16]. This replacement leads to decrease in intensities of characteristic bonds (at 620, 840, 1180, 1250 and 1356 cm^{-1}) of the lead bonds. Further,

these bands disappear with an increase in CuO concentration, probably due to change in the structure of glassy network. However, for the present system, only 0.5 mol% of $CuCl_2$ has been added into the glass matrix and such a small amount of copper may not lead to any significant change in IR spectrum or the structure of the glass.

3.4 Thermal Studies

3.4.1 Thermogravimetric Analysis

Thermal stability of LPCC glass composites was analyzed using nitrogen atmosphere in a temperature range of 25 to 500 °C. It has been realised from the TGA plots that the substitution of CdO into the system does not affect the thermal stability of samples. These samples are found to be well stable up to 500 °C (Fig. 3.5) (Measurements were done to this limit only).

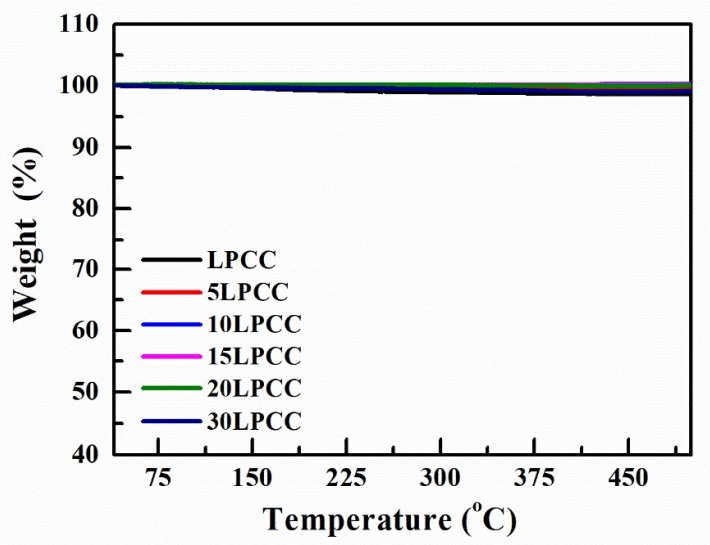

Fig. 3.5 TGA scans for composites of LPCC series.

3.4.2 Differential Scanning Calorimetry

Structural relaxations and crystallization kinetics were explored to understand the thermal behavior of glassy samples. Measurements were performed with variable heating rates (5 - 30 °C/minute). Presence of an endothermic event i.e. T_g marks for structural relaxations in the glass matrix. Exothermic peaks states, crystallization of these samples happens in multiple stages. With the increase in heating rate, thermal events monotonically shift towards higher temperatures (Fig. 3.6 shown for only 30LPCC

composite). Substitution of Pb^{+2} ions by Li^{+} ions in the network increases stiffness (to some extent) in a glassy matrix, which results for increased T_g values. On the other hand, higher concentration of Pb^{+2} ions bring in low T_g values. Similar influences in T_g values by substitution of lead by cadmium are reported [25].

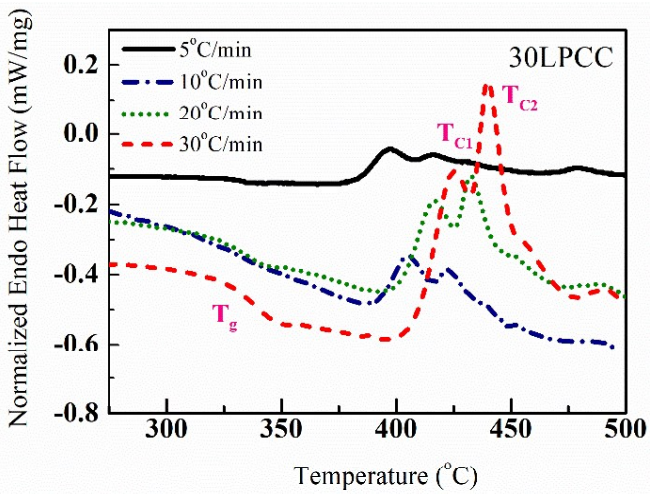

Fig. 3.6 DSC scan of the 30LPCC sample with different scan rates.

From Fig. 3.6, for DSC scan of the 30LPCC composite, it is clearly seen that the crystallization happens in multiple stages. Thermal events like T_g and T_c shifts monotonically with an increase in heating rate. Analysis of the crystallites precipitated and change in their size on heating/annealing the composites up to their point of crystallization temperature has been analyzed from XRD plots of the annealed samples.

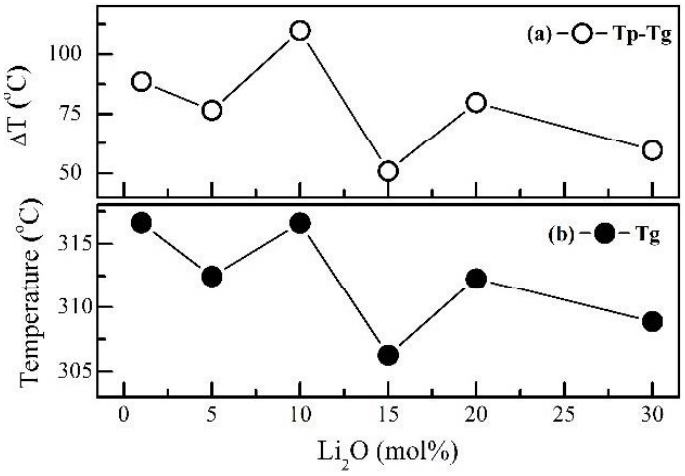

Fig. 3.7 T_g and T_p-T_g for samples of LPCC series.

Thermal data of the glassy samples of this series are further analysed to understand the process of structural relaxations at T_g. A gradual decrease (with a non-linear trend) in T_g can be marked for reduction of the viscous nature of the glass composites on Li_2O substitution (Fig. 3.7).

Stability of samples towards crystallization process has been determined from the T_p-T_g difference. For the LPCC system, a non-linear trend has been observed for these composites for stability towards crystallization process. Overall, these glassy samples are well stable in their glass form as the minimum difference between T_p and T_g is ~50 °C (for 165LPCC composite). Whereas, for rest of the compositions in the LPCC series this difference is more than 50 °C. Thus, these composites are stable to crystallization on heating to higher temperatures.

3.5 Temperature Dependence of Conductivity Cycles

In order to understand the electrical transport during the thermal events and microstructural changes during crystallization in the glassy samples, electrical conductivity measurements have been performed at a frequency of 1 kHz with a function of temperature at a typical heating rate of 1 °C/minute. For the glassy samples, the electrical conductivity measurements for LPCC composites are shown below (Fig. 3.8).

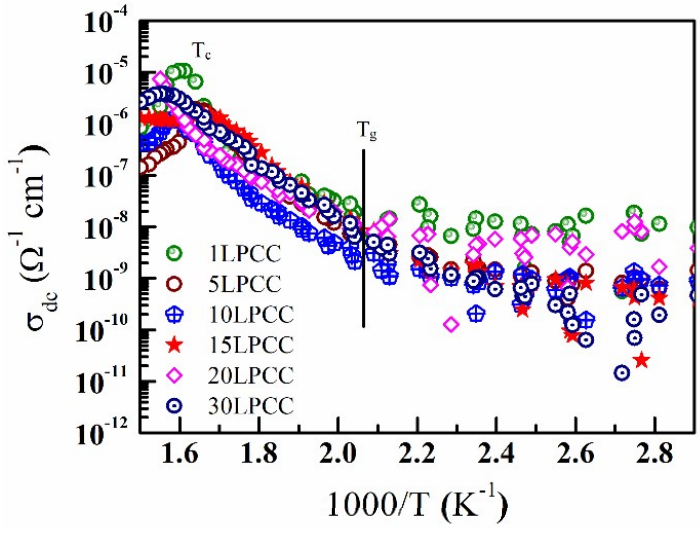

Fig. 3.8 σ-T cycle for composites of LPCC series.

σ-T cycles for these composites can be divided into 2-regions, viz. I and II. Region – I, is a thermally stable region. This region exhibits Arrhenius behavior in electrical conductivity. This cycle can be reversible within a temperature range of $T<T_g$. This region has been used to calculate the activation energy for ion conductions. Region-II is a thermally unstable region. In this region, initially electrical conductivity measurement deviates from linearity and exhibits a remarkable rise, which is related to an increase in free volume of the glass composites due to the presence of glass transition temperature of respective composites. A fall in conductivity of the composites is evident on further increase in temperature, this is because on crossing T_g, the structural relaxations gradually leads to crystallization of the composites. This crystallization process marks for decrease in conductivity of the samples. The conductivity of all the composites (given in table 3.1) has been tabulated in Table 3.3.

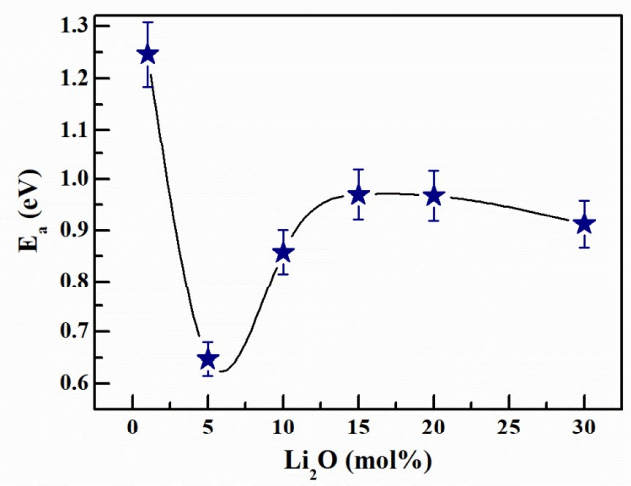

Fig. 3.9 The activation energy for ion transport versus composition.

The activation energy of the ions to transport through the existing channels have been determined from the slope of conductivity measurements (Fig. 3.9). An interesting trend has been observed for change in activation energy along the LPCC composite. As seen from the plot, activation energy initially decreases from LPCC to 5LPCC composites; this could be because of the increase in charge carriers (Li^+ ions) in the composites. However, 10 and 15LPCC composites exhibit an increase in activation energy, which becomes almost constant for later composites. It is because with an increase in the concentration of ions, Li_2O can also participate in glass network formation, however, with further increase in Li^+ ion concentration almost all the available sites for ion

transportation will be occupied and there will not be much energy difference required for ion transportation.

Table 3.3 Conductivity at different temperatures and Activation energy of glass composites.

Sample Code	Conductivity		
	at 305 K	at 523 K	at 573 K
	Ω^{-1} cm^{-1}		
System 3A: xLi_2O-(70-x)PbO-20.5$PbCl_2$-0.5$CuCl_2$ (LPC series)			
1LPC	$\sim10^{-9} - 10^{-10}$	2.5×10^{-7}	4.1×10^{-6}
5LPC	$\sim10^{-9} - 10^{-10}$	1.6×10^{-7}	1.3×10^{-6}
10LPC	$\sim10^{-9} - 10^{-10}$	2.7×10^{-7}	4.1×10^{-6}
15LPC	-	-	-
20LPC	$\sim10^{-9} - 10^{-10}$	1.9×10^{-6}	1.0×10^{-5}
40LPC	$\sim10^{-9} - 10^{-10}$	2.4×10^{-6}	2.1×10^{-5}
System 3B: xCdO-(80-x)PbO-20$PbCl_2$; (CPP series)			
PP	$\sim10^{-9} - 10^{-10}$	2.8×10^{-7}	1.5×10^{-6}
5CPP	$\sim10^{-9} - 10^{-10}$	3.8×10^{-5}	9.4×10^{-5}
10CPP	$\sim10^{-9} - 10^{-10}$	8.8×10^{-8}	6.8×10^{-7}
15CPP	-	-	-
20CPP	-	-	-
30CPP	$\sim10^{-9} - 10^{-10}$	5.1×10^{-8}	2.4×10^{-7}
System 3C: xCdO- (80-x)PbO-19$PbCl_2$-$CuCl_2$; (CPPC series)			
PPC	$\sim10^{-8} - 10^{-9}$	6.7×10^{-8}	1.8×10^{-7}
5CPPC	-	-	-
10CPPC	-	-	-
15CPPC	$\sim10^{-8} - 10^{-9}$	2.5×10^{-6}	1.8×10^{-5}
20CPPC	$\sim10^{-8} - 10^{-9}$	6.7×10^{-8}	4.6×10^{-7}
30CPPC	-	-	-
System 3D: xLi_2O-(50-x)PbO-19$PbCl_2$-30CdO-$CuCl_2$; (LPCC series)			
LPCC	$\sim10^{-9} - 10^{-10}$	5.5×10^{-8}	2.4×10^{-7}
5LPCC	$\sim10^{-9} - 10^{-10}$	2.8×10^{-8}	2.3×10^{-7}
10LPCC	$\sim10^{-9} - 10^{-10}$	1.9×10^{-8}	7.3×10^{-8}
15LPCC	$\sim10^{-9} - 10^{-10}$	4.8×10^{-8}	5.8×10^{-7}
20LPCC	$\sim10^{-9} - 10^{-10}$	2.8×10^{-8}	1.6×10^{-7}
30LPCC	$\sim10^{-9} - 10^{-10}$	4.8×10^{-8}	4.2×10^{-7}

3.6 Conclusions

Lead oxyhalide glasses were doped with Li^+ ions and Cd^{2+} ion in the glass matrix. These composites were explored for ionic conduction. Investigations of these composites indicated that these composites exhibit very poor ionic conductivity (~10^{-9}-10^{-10} Ω^{-1} cm^{-1}) at room temperature as well as at high temperature (~10^{-9}-10^{-7} Ω^{-1} cm^{-1}). In a few cases we see the conductivity of the order 10^{-5} Ω^{-1} cm^{-1} (Table 3.3). However, we are not sure of getting the same result for repeated heating cycles as crystallization may set in. Spectroscopic investigations of these composites indicate that as they are IR transparent, they could be employed for photonic device applications and the presence of lead would make them useful for radiation shielding applications.

Our main aim was to design an electrolyte with high ionic conductivity for solid-state device applications. Investigations on lead oxyhalide glassy systems did not show interesting conductivity results. It is not impossible to produce good ionic conductors in these systems; one may require introducing appropriate f-block metal ions carefully in the system along with lithium ion and fine tuning of composition is to be done. Also, this process of preparing the electrolyte is a high temperature process and f-block metal ions will bring in issues such as the cost and availability for mass production. Therefore, we shifted our attention to sol-gel processed silica-gel solid electrolytes with reasonably good conductivity and stability. The preparation of these composites was comparatively easier and done at low temperature. The explored silica-gel systems have been thoroughly discussed in chapter 4.

References

1. Vishwanath P. Singh, N.M. Badiger, J. Kaewkhao, "Radiation shielding competence of silicate and borate heavy metal oxide glasses: Comparative study", *Journal of Non-Crystalline Solids* **404** (2014) 167–173.
2. El Egili K., Doweidar H., Moustafa Y., Abbas I., "Structure and some physical properties of $PbO-P_2O_5$ glasses", *Physica B: Condensed Matter* **339** (2003) 237-245.
3. Rada S., Pascuta P., Culea M., Maties V., Rada M., Barlea M., Culea E., "The local structure of europium-lead-borate glass ceramics", *Journal of Molecular Structure.* **924** (2009) 89-92.
4. El Damarawi G., "Influence of $PbCl_2$ on physical properties of lead chloroborate glasses", *Journal of Non-Crystalline Solids* **176** (1994) 91-97.
5. Sokolov I. A., Murin I. V., Wiemhöfer H. D., Pronkin A. A., "The nature of current carriers and electric conductivity in the $PbCl_2$-2PbO-SiO_2 glasses", *Glass Physics and Chemistry.* **26** (2000) 148-157.
6. Rao B. G., Sundar H. K., Rao K. J., "Investigations of glasses in the system PbO-PbF_2", *Journal of the Chemical Society, Faraday Transactions I* **80** (1984) 3491-3501.
7. Rao K. J., Rao B. G., Elliott S., "Glass formation in the system PbO-$PbCl_2$", *Journal of Material Science* **20** (1985) 1678-1682.
8. Pan Z., Henderson D. O., Morgan S. H., "A Raman investigation of lead halo borate glasses", *The Journal of Chemistry Physics* **101** (1994) 1767-1774.
9. Gressler C. A., Shelby J. E., "Lead fluoroborate glasses", *Journal of Applied Physics* **64** (1988) 4450-4453.
10. Chetana B., Viswanatha R., Reddy C. N., Rao K. J., "Thermal and spectroscopic investigations of glasses in the system PbO-$PbCl_2$-$PbBr_2$", *Physics and Chemistry of Glasses: European Journal of Glass Science and Technology B,* **56** (2015) 115-120.
11. Lezal D., Pedlikova J., Kostka P., Bldska J., Poulain M., Zavadil J., "Heavy metal oxide glasses: Preparation and physical properties", *Journal of Non-Crystalline Solids* **284** (2001) 288-295.

12. Wagh A., Petwal V., Verma V. P., Dwivedi J., Raviprakash Y., Kamath S. D., "Electron beam irradiation on lead fluoroborate glasses doped by europium ions", *Journal of Thermal Analysis and Calorimetry* **124** (2016) 619-628.

13. Wang Y., Osaka A., Miura Y., "Anionic conduction in lead oxyhalide glasses", *Journal of Non-Crystalline Solids* **112** (1989) 323-327.

14. Sokolov I., Murin I., Mel'nikova N., Pronkin, "A study of ionic conductivity of glasses in the $PbCl_2$-PbO-B_2O_3 and $PbCl_2$-2PbO-B_2O_3 systems", *Glass Physics and Chemistry* **29** (2003) 291-299.

15. Montagne L., Donze S., Palavit G., Boivin J., Fayon F., Massiot D., Grimblot J., Genegembre L., "207Pb and 113Cd NMR and XPS characterization of PbO-$PbCl_2$-$CdCl_2$ glasses." *Journal of Non-Crystallization Solids* **293** (2001) 74-80.

16. Kashif I., Ratep A., "Effect of copper oxide on structure and physical properties of lithium lead borate glasses", *Applied Physics A* **120** (2015) 1427-1434.

17. Alemi A., Sedghi H., Mirmohseni A., Golsanamlu V., "Synthesis and characterization of cadmium doped lead-borate glasses", *Bulletin of Materials Science* **29** (2006) 55-58.

18. Jie F., Yatsuda H., "Glass formation in the system PbO-$PbCl_2$-$CdCl_2$", *Journal of Materials Science Letters* **14** (1995) 580-581.

19. Siidra O., Krivovichev S., Teske C., Depmeier W., "Synthesis and crystal structure of a new oxohalide $CdPb_2O_2Cl_2$", *Glass Physics and Chemistry* **35** (2009) 411-415.

20. Chahine A., Et-Tabirou M., Elbenaissi M., Haddad M., Pascal J., "Effect of CuO on the structure and properties of (50-x/2)Na_2O-xCuO-(50-x/2)P_2O_5 glasses", *Materials Chemistry and Physics* **84** (2004) 341-347.

21. P. Raghunathan, S. C. Sivasubramanian, "X-ray Diffraction, Electron Paramagnetic Resonance, and Electron Spin Echo Modulation Studies of the PbO-$PbCl_2$,-$CuCl_2$, Ternary Glass System", *Journal of Physical Chemistry*, **95** (1991) 6346-6351.

22. P. Raghunathan, S.C. Sivasubramanian, "Structural Characterization of Some Novel Ternary PbO-$PbCl_2$-$CuCl_2$ Glasses by X-Ray Pair Distribution Functions, Thermal Analysis and Electron Paramagnetic Resonance", *Journal of Non-Crystalline Solids* **136** (1991) 14-26.

23. Dayanand C., Bhikshamaiah G., Salagram M., "IR and optical properties of PbO glass containing a small amount of silica", *Materials Letters* **23** (1995) 309-315.

24. Kurushkin M., Semencha A., Blinov L., Mikhailov M., "Lead-containing oxyhalide glass." *Glass Physics and Chemistry* **40** (2014) 421-427.

25. Silva M., Briois V., Poulain M., Messaddeq Y., Ribeiro S., "Lead-cadmium oxyfluoride glasses and glass-ceramics." *Journal of Optoelectronics and Advanced Materials* **4** (2002) 799-808.